Proton Structure at High Q^2

E.-E. Woehrling[a]

[a]School of Physics and Space Research, University of Birmingham, Edgbaston, Birmingham B152TT, UK

The results of inclusive charged and neutral current measurements at HERA are shown. The results cover a Q^2 range of 100 to 30 000 GeV^2 and Bjorken x between 0.0013 and 0.65. Measurements of the proton structure functions $\tilde{F}_2$ and $x\tilde{F}_3$ are made, as well as the extraction of $\tilde{F}_L$ in the range 110 < Q^2 <700 GeV^2. Parton distribution functions are extracted from these data in a next to leading order QCD analysis.

1. Introduction

The ep collider, HERA, has been running in both e^+p and e^-p modes from 1998 to 2000, obtaining luminosities of $\sim$100pb^{-1} and 16pb^{-1}, respectively, at a centre of mass energy of $\sqrt{s} \sim 320$ GeV^2. H1 and ZEUS have used these large data sets to measure neutral and charged cross sections, and to determine the structure functions of the proton. By combining the neutral current and charged current information, a theoretical undestanding of parton distribution functions (PDFs) has been achieved.

The cross sections are defined in terms of the kinematic variables Q^2, Bjorken x, and y. Q^2 is the negative squared 4-momentum transfer of the exchanged boson. It is appropriate to think of Bjorken x as the fraction of the proton momentum carried by the struck quark in the proton's infinite momentum frame, and y as the fraction of the electron momentum carried by the exchanged boson in the proton's rest frame.

2. Neutral Current Interactions

The single differential neutral current cross section (Fig. 1) shows a strong Q^2 dependance, with a similar trend for e^-p and e^+p data up to $Q^2 \sim$ M$_Z^2$. This follows the $1/Q^4$ dependency predicted by the standard model, as expressed in equation (1) [1–3]:

$$\frac{d^2\tilde{\sigma}(e^{\mp}p)}{dx\,dQ^2} = \quad (1)$$
$$\frac{2\pi\alpha^2}{xQ^4}\left[Y_+\tilde{F}_2(x,Q^2) - y^2\tilde{F}_L(x,Q^2) \pm Y_- x\tilde{F}_3(x,Q^2)\right],$$

where $Y_\pm(y) = 1 \pm (1-y)^2$, and $\tilde{F}_2$, $x\tilde{F}_3$ and $\tilde{F}_L$ are the generalised proton structure functions.

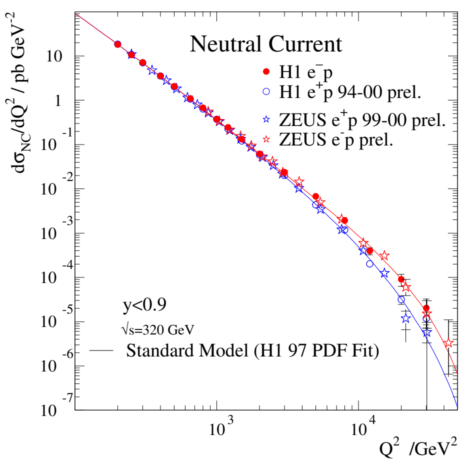

Figure 1. The neutral current cross section, single differential in Q^2.

$\tilde{F}_2$ is the dominant term for a large range in Q^2 and is sensitive to all quark and anti-quark types, $\tilde{F}_2 \propto \sum(q_i + \bar{q}_i)$. $x\tilde{F}_3$ is a Z^0 dependent component of the exchange, and is only significant at high Q^2 ($Q^2 \simeq M_Z^2$). $x\tilde{F}_3$ is of particular interest since it is sensitive to the valence quarks,

$x\tilde{F}_3 \propto \sum(q_i - \bar{q}_i)$. Finally, $\tilde{F_L}$ is a NLO (next to leading order) term, which represents the coupling between the proton and longitudinally polarised virtual photons. $\tilde{F_L}$ is strongly dependent on the gluonic content of the proton, and only contributes significantly to the cross section at high y due to the y^2 weighting in equation (1).

The reduced neutral current cross section may be obtained from equation (1) by drawing the kinematic factors into the reduced cross section definition:

$$\tilde{\sigma}^{\pm}_{NC} \equiv \left[\tilde{F}_2 \mp \frac{Y_-}{Y_+} x\tilde{F}_3 - \frac{y^2}{Y_+}\tilde{F}_L\right] \qquad (2)$$

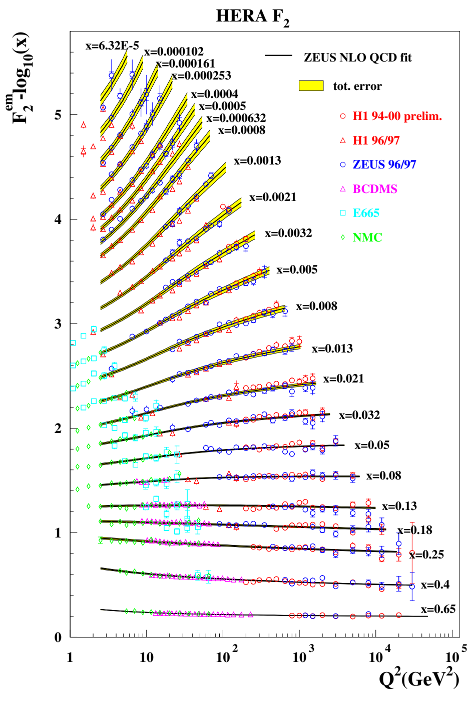

Figure 2. The proton structure function F_2, plotted as a function of Q^2 for various values of x.

The generalised structure functions are comprised of structure functions that differentiate between pure γ, γZ^0 interference and pure Z^0 exchange. In the case of $\tilde{F}_2$ the F_2, pure γ, term dominates due to small multiplicative factors that are applied to the ${F_2}^{\gamma Z^0}$ and ${F_2}^{Z^0}$ terms. In the case of $x\tilde{F}_3$ there is no pure γ contributing term, and the dominant term is $x{F_3}^{\gamma Z^0}$.

3. $\tilde{F}_2$

Figure 2 shows F_2, the dominant term in the neutral current cross section, calculated from both H1 and ZEUS datasets, as well as from fixed target data. The dependence of F_2 on Q^2 is an effect called scaling violation, which is the result of gluon radiation. There is a good agreement between H1 and ZEUS, as well as between HERA and fixed target experiments. F_2 is well described by a NLO QCD fit using the DGLAP evolution over four orders of magnitude in both Q^2 and x [4,5].

4. $x\tilde{F}_3$

$x\tilde{F}_3$ is measured by subtracting the e^+p neutral current cross section from that obtained from e^-p scattering data (equation (2)). Although the measurement is statistically limited, due to the fact that $x\tilde{F}_3$ only becomes significant at $Q^2 \simeq \mathrm{M}_Z^2$, there are enough data for a measurement. The result of which is shown in Fig. 3. The HERA $x\tilde{F}_3$ measurements are also reasonably well described by the NLO QCD fit [1,3].

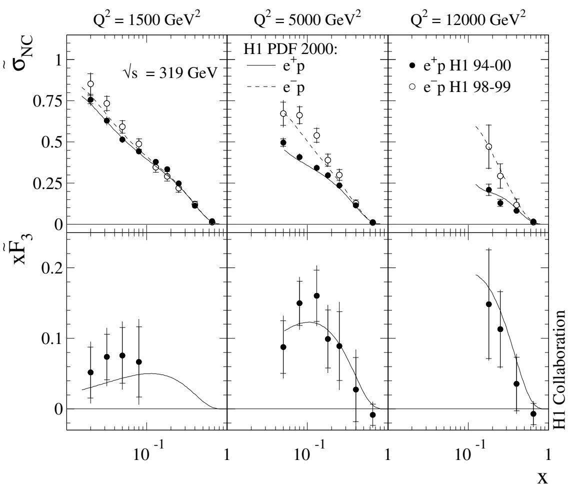

Figure 3. Measurement of the structure function $x\tilde{F}_3$. Also shown are the results of a NLO QCD fit to the data.

$x\tilde{F}_3$ can be divided into γ-Z^0 interference and Z^0 only contributions,

$$x\tilde{F}_3 \equiv -a_e \frac{\kappa_w Q^2}{Q^2+M_Z^2} xF_3{}^{\gamma Z^0} + (2v_e a_e)\left[\frac{\kappa_w Q^2}{Q^2+M_Z^2}\right]^2 xF_3{}^{Z^0}. \tag{3}$$

As v_e and the propagator terms are both very small ($v_e \sim 0.05, \frac{\kappa_w Q^2}{Q^2+M_Z^2} \leq 0.5$), $xF_3{}^{\gamma Z^0} >> xF_3{}^{Z^0}$, it is possible to neglect $xF_3^{Z^0}$ and extract the dominant term, $xF_3^{\gamma Z^0}$.

Figure 4 shows $xF_3^{\gamma Z^0}$ from ZEUS and fixed target (BCDMS) experiments. The measurements are consistent despite an order of magnitude difference in Q^2. The HERA statistical limitation is due to the small amount of e^-p data, and will be reduced with further e^-p data taking.

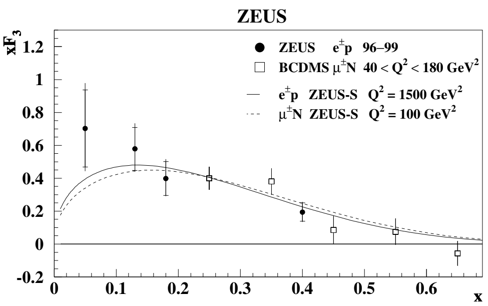

Figure 4. $xF_3^{\gamma Z^0}$ plotted against x with data points and standard model expectation from both the BCDMS and ZEUS experiments.

5. $\tilde{F}_L$

F_L cannot be directly determined from HERA data until data is taken with a different centre of mass energy. The data is, however, sensitive to F_L at high y (see eq 1), and it is possible to extract F_L by taking the approach that $\tilde{F}_2$ is well determined over a wide range of x and Q^2, and thus can be extrapolated to high y using the DGLAP equation [2]. Thus, by subtracting the $\tilde{F}_2$ term, and making a correction for $x\tilde{F}_3$ (a minor effect as F_L is extracted at low Q^2 and high y) it is possible to determine a value for F_L from the measured cross section.

Figure 5 shows the results of the extraction of F_L over a range of Q^2 (and thus also x) at a fixed value of y (=0.75). Both e^-p and e^+p data are shown, and it can be seen that the e^-p and e^+p data are matched by the predicted NLO QCD fit, and are inconsistent with both the theoretical limits F_L=0 and F_L=F_2. The F_L extraction is an important test of the consistency of QCD, since F_L only arises through higher order corrections. Measurements have also been made at lower Q^2 which are also well described by the theory [4].

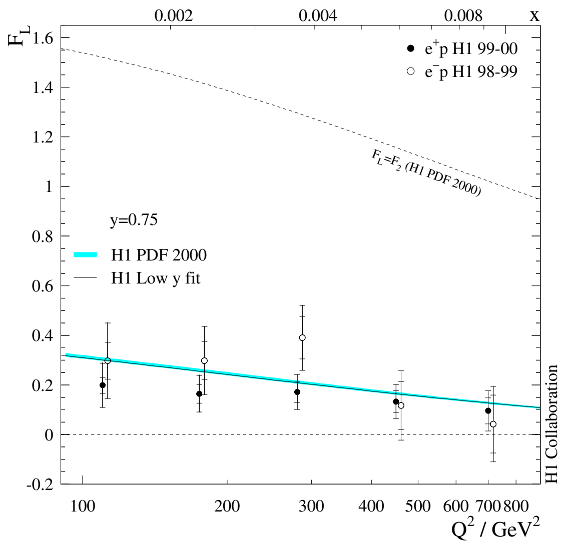

Figure 5. The H1 extraction of the structure function F_L.

6. Charged Current Interactions

The charged current reaction (ep $\rightarrow \nu$X) is described by the equation

$$\frac{d^2\tilde{\sigma}_{CC}(e^{\pm}p)}{dx\, dQ^2} = \tag{4}$$

$$\frac{G_F^2}{4\pi x}\left[\frac{M_W^2}{Q^2+M_W^2}\right](Y_+ W_2^{\pm} \mp Y_- xW_3^{\pm} - y^2 W_L^{\pm})$$

where the charged current structure functions $W_2^{\pm}$, $xW_3^{\pm}$ and $W_L^{\pm}$ are defined in a similar way to the neutral current structure functions. In the

Quark Parton Model (where $W_L^{\pm} \equiv 0$), the structure functions can be defined in terms of sums and differences in the quark and anti-quark distributions.

Similarly to neutral current interaction, the charged current interaction can be described in terms of a reduced cross section:

$$\tilde{\sigma}_{CC}^{+} = x \cdot \left[\bar{u} + \bar{c} + (1-y)^2 (d+s)\right] \tag{5}$$

in the case of positron scattering, and the equation

$$\tilde{\sigma}_{CC}^{-} = x \cdot \left[u + c + (1-y)^2 (\bar{d}+\bar{s})\right] \tag{6}$$

in the case of electron scattering.

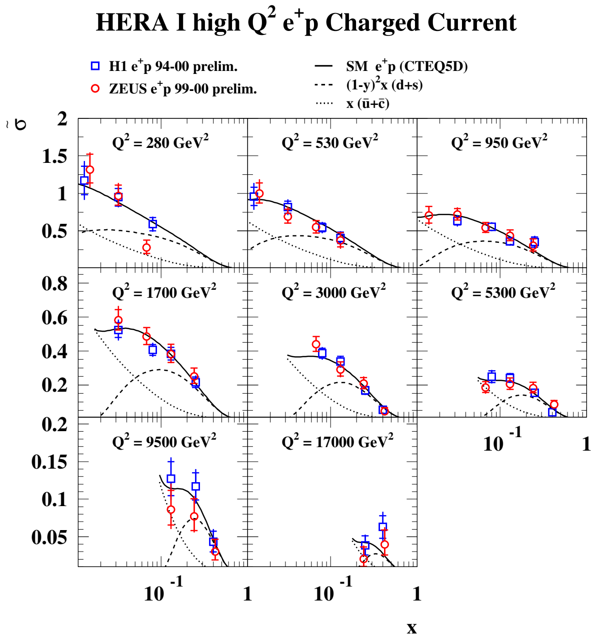

Figure 6. H1 and ZEUS measurements of the charged current cross section from positron data are plotted as the points (squares and circles respectively). The full line is a CTEQ QCD fit [6], the dashed line is the D-type quark contribution, and the dotted line is the $\bar{\mathrm{U}}$ $(\bar{\mathrm{u}}+\bar{\mathrm{c}})$ contribution. It is observed that at high x, the D type contribution dominates, while at low x, the $\bar{\mathrm{U}}$ contribution dominates.

Thus we see that the e^+p charged current interaction, at high x (low y), probes the d quark composition of the proton, while the e^-p interaction probes the u quarks. It is important to remember that it is not possible to distinguish between valance and sea quarks in this interaction, however, at high x, the valence quarks dominate the proton structure. The U type (u+c) quark distribution is generally obtained from neutral current interactions, so the positron charged current interaction is most interesting for the insight gained for the D type (d+s) structure of the proton. This information, combined with the neutral current results, is used to extract the PDFs.

7. PDFs

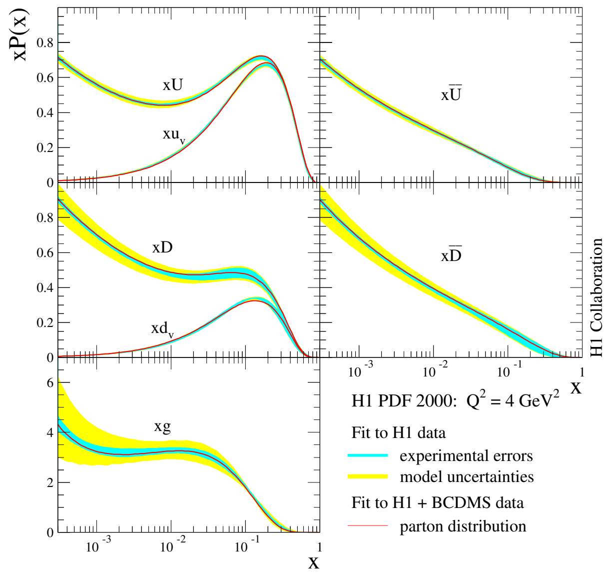

Figure 7. The xU, $x\bar{\mathrm{U}}$, xD, $x\bar{\mathrm{D}}$ and xg parton distributions as determined from the H1 PDF 2000 fit to H1 data alone. The distributions are shown at Q^2 of 4 GeV^2 with experimental and model uncertainties. For comparison the central values from the fit to H1 and BCDMS data are also shown (the full curve).

H1 and ZEUS each use a different method to determine the PDFs [1,7]. H1 uses only H1 data (cross-checking with fixed target, BCDMS, data) while ZEUS have both a ZEUS only fit (ZEUS-o) and a ZEUS plus fixed target fit (ZEUS-s). For the first time, HERA-only fits (Fig. 7) can prove their competitiveness with world data. At high x, the errors on the PDFs are experimentally dominated, while at low x the errors are typically dominated by the theoretical model uncertainties. Fig. 8 shows the ZEUS-s fit, which is compared to the results of the CTEQ and MRST fits.

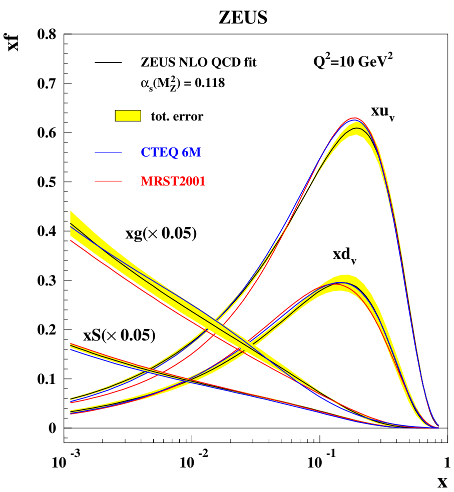

Figure 8. The $xu_{\rm v}$, $xd_{\rm v}$, xS (sea) and xg distributions determined from the ZEUS-s fit, using ZEUS and fixed-target data, shown here at Q^2 of 10 GeV^2. The results of the CTEQ and MRST fits are also plotted for comparison.

H1 also performs a local extraction of the u and d content of the proton [1]. This is only done at high x, where the u and d quarks carry more than 70% of the proton's momentum. The systematic errors of this extraction differ to that of the QCD fit and, although the fit errors are taken into account, they mostly cancel. The extraction is therefore less sensitive to assumptions made in other regions of phase space. Fig. 9 shows the results of this extraction, with the extracted values plotted as points and the lines showing the H1 PDF fit.

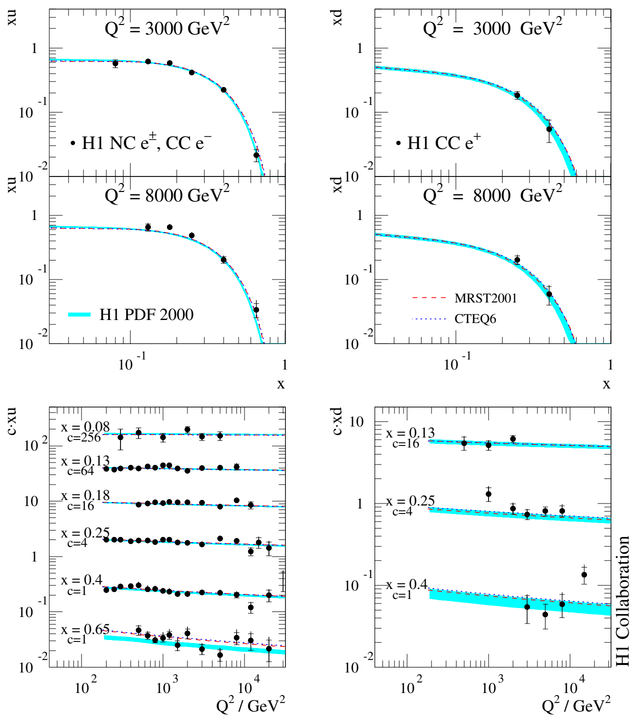

Figure 9. Local extraction of the proton u and d content. The local extraction is plotted as points, while the H1 PDF 2000 fit is plotted as a band and MRST and CTEQ predictions are shown as dashed and dotted lines respectively.

REFERENCES

1. H1 Collab., C. Adolff et al., DESY 03-038 (March 2003) submitted to Eur. Phys. J.
2. H1 Collab., abstract 978, paper submitted to ICHEP02 Conferance, Amsterdam
3. ZEUS Collab, S. Chekanov et al., Eur. Phys. J. C28(2003) 2,175-201
4. H1 Collab., C. Adolff et al., Eur. Phys. J.C21(2001) 33-61
5. ZEUS Collab, S. Chekanov et al., Eur. Phys. J. C21(2001) 3,443-471
6. J. Pumplin et al., JHEP 0207 (2002) 012
7. ZEUS Collab, S. Chekanov et al., Phys. Rev. D67, 012007 (2003)